This article was downloaded by:
On: *25 January 2011*
Access details: *Access Details: Free Access*
Publisher *Taylor & Francis*
Informa Ltd Registered in England and Wales Registered Number: 1072954 Registered office: Mortimer House, 37-41 Mortimer Street, London W1T 3JH, UK

Separation Science and Technology
Publication details, including instructions for authors and subscription information:
http://www.informaworld.com/smpp/title~content=t713708471

Effects of the Residence Time in Four-Bed Pressure Swing Adsorption Process

Se-Il Yang[a]; Ju-Yong Park[a]; Dae-Ki Choi[a]; Sung-Hyun Kim[b]
[a] Energy and Environment Research Division, Korea Institute of Science and Technology, Cheongryang, Seoul, Korea [b] Department of Chemical and Biological Engineering, Korea University, Seoul, Korea

To cite this Article Yang, Se-Il , Park, Ju-Yong , Choi, Dae-Ki and Kim, Sung-Hyun(2009) 'Effects of the Residence Time in Four-Bed Pressure Swing Adsorption Process', Separation Science and Technology, 44: 5, 1023 — 1044
To link to this Article: DOI: 10.1080/01496390902729122
URL: http://dx.doi.org/10.1080/01496390902729122

PLEASE SCROLL DOWN FOR ARTICLE

Full terms and conditions of use: http://www.informaworld.com/terms-and-conditions-of-access.pdf

This article may be used for research, teaching and private study purposes. Any substantial or systematic reproduction, re-distribution, re-selling, loan or sub-licensing, systematic supply or distribution in any form to anyone is expressly forbidden.

The publisher does not give any warranty express or implied or make any representation that the contents will be complete or accurate or up to date. The accuracy of any instructions, formulae and drug doses should be independently verified with primary sources. The publisher shall not be liable for any loss, actions, claims, proceedings, demand or costs or damages whatsoever or howsoever caused arising directly or indirectly in connection with or arising out of the use of this material.

Separation Science and Technology, 44: 1023–1044, 2009
Copyright © Taylor & Francis Group, LLC
ISSN: 0149-6395 print/1520-5754 online
DOI: 10.1080/01496390902729122

Taylor & Francis
Taylor & Francis Group

Effects of the Residence Time in Four-Bed Pressure Swing Adsorption Process

Se-Il Yang,[1] Ju-Yong Park,[1] Dae-Ki Choi,[1] and Sung-Hyun Kim[2]
[1]Energy and Environment Research Division, Korea Institute of Science and Technology, Cheongryang, Seoul, Korea
[2]Department of Chemical and Biological Engineering, Korea University, Seoul, Korea

Downloaded At: 09:02 25 January 2011

Abstract: Hydrogen separation by the four-bed PSA process using layered beds of activated carbon and zeolite 5A was investigated experimentally and theoretically to recover high purity H_2 from steam methane reforming off-gas. The recovery increased with increasing the residence time at given product purity because of the contact time between the impurities and the adsorbents is increased. The difference of increasing the recovery became smaller with increasing the residence time and then the recovery was not increased after 43.6 seconds of the residence time. The minimum residence time exists to obtain the maximum recovery at desired product purity (99.999%+).

Keywords: Hydrogen, pressure swing adsorption, residence times

INTRODUCTION

Hydrogen, regarded as an ecologically clean and renewable energy source, is increasingly demanded in various fields including fuel cells, semiconductor processing, and the petrochemical industry. The most common commercial method for the production of hydrogen is the reformation of natural gas (methane) by reaction with steam. The steam reforming

Received 25 August 2008; accepted 20 December 2008.
Address correspondence to Se-Il Yang, Energy and Environment Research Division, Korea Institute of Science and Technology, P. O. Box 131, Cheongryang, Seoul 130-650, Korea. Tel.: +82-2-958-5885; Fax: +82-2-958-5205. E-mail: yseil78@kist.re.kr

off-gas is composed of about 70∼75% hydrogen, 20% carbon dioxide, 3% carbon monoxide, 4% methane, and small amounts of water. The current technology to separate hydrogen from steam reforming off-gas is pressure swing adsorption (PSA). The resulting hydrogen-rich gas (70∼75% H_2) is then purified to produce a 99.99% + H_2 stream by a PSA process (1–3).

PSA is a well-known method for the separation of bulk gas mixtures and for the purification of gas streams containing undesirable impurities. There has been a tremendous growth in PSA during the past four decades through the modification of the established process and the development of new adsorbents (4). Hence, the final separation in new hydrogen-producing plants is based on PSA utilizing the difference in adsorption properties of various molecules; e.g., components of a gas mixture are selectively adsorbed onto a solid matrix at high pressure and subsequently desorbed by lowering the pressure. A great deal of PSA process concepts have been patented in the last thirty years, several of which have been commercialized (5).

Downloaded At: 09:02 25 January 2011

As hydrogen is separated from steam reforming off-gas using the PSA process, layered beds consisting of different adsorbents, such as activated carbon and zeolite, have been used. Typically carbon dioxide and a part of methane and carbon monoxide are adsorbed on the first layer of activated carbon while methane and carbon monoxide are adsorbed on the second layer of zeolite (2). The performance in the PSA process is usually defined as the purity and recovery of hydrogen obtained by executing both experiments and mathematical modelling. The high purity and recovery of the H_2 PSA processes are largely due to an effective operation of multi-bed PSA processes including several pressure equalizations, backfill, and layered adsorption bed.

The design and operation of this PSA process is complex because of the large number of variables and parameters involved. Most pervious studies on PSA design have been made through rigorous modelling and experimental investigation (6). The economic production of high purity hydrogen requires low operating and capital costs, whereas the capital costs depend largely upon the size of the vessels containing the PSA adsorbent beds. The PSA bed size is determined by the desired hydrogen productivity and purity. Hydrogen productivity and recovery are increased by improved process cycles and/or improved adsorbents. The design methods of the bed size need to reduce overall capital costs, for improved hydrogen recovery.

In the present study, hydrogen separation by the PSA process using the layered beds of activated carbon and zeolite 5A was investigated experimentally and theoretically to recover high purity H_2 from steam reforming off-gas. Aspen Adsim (Aspen Tech, Inc.) was then utilized for the estimation and the simulation of the PSA process cycles. The

simulation results obtained were analyzed numerically by using a non-isothermal dynamic model incorporating mass, energy, and momentum balance. By combining the experimental results and the simulation results, we consequently suggest a design factor of the PSA bed size for maximizing recovery at the desired hydrogen purity.

EXPERIMENT

In this study, the adsorbents used activated carbon (Granular type, $6 \sim 16$ mesh) and zeolite 5A (Sphere type, $4 \sim 8$ mesh). The activated carbon was supplied by Calgon Corporation with an average pellet size of 1.15 mm. The zeolite 5A was supplied by W. R. Grace Corporation with an average pellet size of 1.57 mm. The physical properties of the adsorbents and bed are listed in Table 1. Before the experiment, the adsorbents were regenerated for more than 24 hours at 573 K in a drying vacuum oven. The feed composition based on the steam methane reforming (SMR) off-gas (72.2 vol% H_2, 21.6 vol% CO_2, 2.03 vol% CO, 4.17 vol% CH_4) was used. It was assumed that water and other pollutants were pre-treated before being fed into the PSA process.

The schematic diagram of the experimental apparatus is shown in Fig. 1. The four adsorption beds were made of stainless steel 3.84 cm

Downloaded At: 09:02 25 January 2011

Table 1. Physical properties of adsorbents and bed

		Activated carbon	Zeolite 5A
Adsorbents			
Average pellet size	(mm)	1.15	1.57
Pellet density	(g/cm^3)	0.85	1.16
Bulk density	(g/cm^3)	0.482	0.764
Heat capacity	($cal/g \cdot K$)	0.25	0.21
Bed			
Length	(cm)	100	70
Inside diameter	(cm)	3.84	
Outside diameter	(cm)	4.86	
Heat capacity of column	($cal/g \cdot K$)	0.12	
Internal heat transfer coefficient	($kJ/s \cdot m^3 \cdot K$)	0.0385	
External heat transfer coefficient	($kJ/s \cdot m^3 \cdot K$)	0.0142	
Density of column	(g/cm^3)	7.83	
Bulk density	(g/cm^3)	0.532	0.744
External void fraction	(-)	0.433	0.357

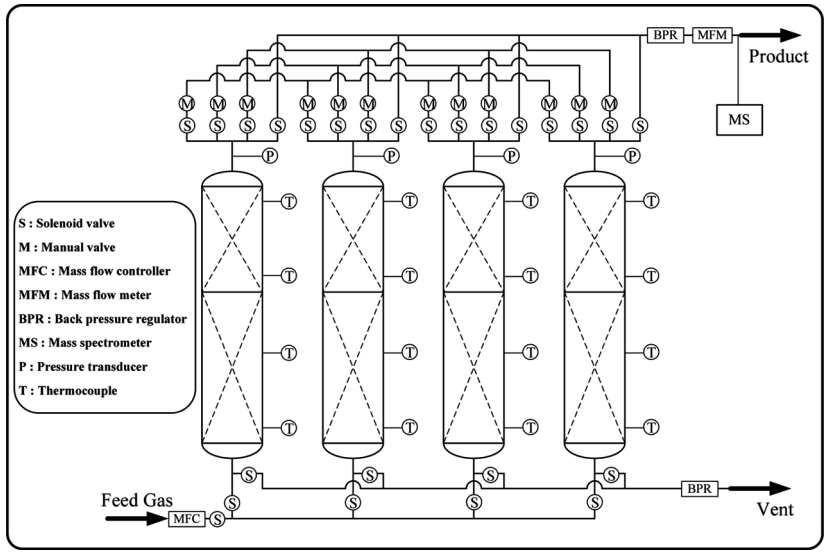

Figure 1. Schematic diagram of four-bed PSA process.

Downloaded At: 09:02 25 January 2011

ID, 170 cm length, and 0.51 cm wall thickness and packed with activated carbon and zeolite 5A. The activated carbon layer height is 100 cm at the feed end and the zeolite 5A layer height is 70 cm above the activated carbon layer. To measure the temperature inside the bed, four thermocouples (K type) were installed at each of the four beds and located in the bed at 10, 60, 110, and 160 cm distant from the top of the packed section, at the center and at half the bed radius. The pressure transducers (Sensys Tech.) were installed at the top of each bed in order to measure the pressure profile. The pre-calibrated mass flow controller (Bronkhorst High-Tech) by a wet gas meter (Shinagawa) was installed to control the feed rate. The adsorption pressure and the purge pressure in the bed were controlled by the electrical back pressure regulators. The pre-calibrated mass flow meter (Bronkhorst High-Tech) by a wet gas meter (Shinagawa) was installed to measure the product flow rate. The sampling port was placed downstream of the mass flow meter, so that the product flow rate could be measured without any loss due to sampling. The product concentrations were monitored continuously and automatically with a mass spectrometer (Omnistar 300). The control of the solenoid valve switching and the data acquisition of measuring variables were done by a PLC (National Instruments) linked to a personal computer whose monitor provided an on-line display of dynamic changes in all measured values.

PSA PROCESS DESCRIPTION

To obtain high-purity hydrogen from SMR off-gas, a four-bed, a ten-step PSA process cycle was experimented with and simulated. The PSA process designed for this study consisted of the following steps (7–11):

(a) Adsorption (AD): Feed gas is passed at adsorption pressure P^F(9 atm) through an adsorber and a pure H_2 stream is produced through the product end at the feed gas pressure.
(b) Adsorption and Provide Pressurization (AD and PP): Feed gas is passed at adsorption pressure through an adsorber and a pure H_2 stream is produced through the product end at the feed gas pressure. A part of this gas was used for pressurization of a companion bed (step (j)).
(c) First Pressure Equalization (EQI-BD): The bed is cocurrently depressurized to a pressure level of P^1. Pure H_2 is produced through the product end which is utilized to partially pressurize another bed undergoing step (i).
(d) Provide Purge (PP): The bed is cocurrently depressurized to a pressure level of P^2. The effluent gas in this step is used to purge another bed undergoing step (g).
(e) Second Pressure Equalization (EQII-BD): The bed is further depressurized cocurrently to a pressure level of P^3. The effluent gas through the product end, that is, a high purity H_2, is used to pressurize another bed undergoing step (h).
(f) Blow down (BD): The bed is countercurrently depressurized to the lowest pressure level of cycle (P^4). The effluent gas, which contains a part of the desorbed gases and most of the bed void gases, is wasted.
(g) Purge (PG): The bed is countercurrently purged with pure H_2 at pressure P^4 obtained from a bed undergoing step (c). The effluent gas in this step contains the remains of the desorbed impurities, which are then wasted.
(h) Second Pressure Equalization (EQII-PR): The bed is pressurized from pressure P^4 to P^5 by countercurrently introducing the gas produced by a bed undergoing step (e).
(i) First Pressure Equalization (EQI-PR): The bed is further pressurized from P^5 to P^6 by countercurrently introducing the effluent gas from step (c).
(j) Backfill (BF): Finally, The bed pressure was raised from P^6 to P^F by introducing a part of the H_2 product gas from a bed undergoing step (b). The bed is now ready for the next cycle from step (a) to step (j).

Figure 2 shows the pressure history for the above-mentioned PSA process and Table 2 presents the cycle steps and time schedules. The impurities

Downloaded At: 09:02 25 January 2011

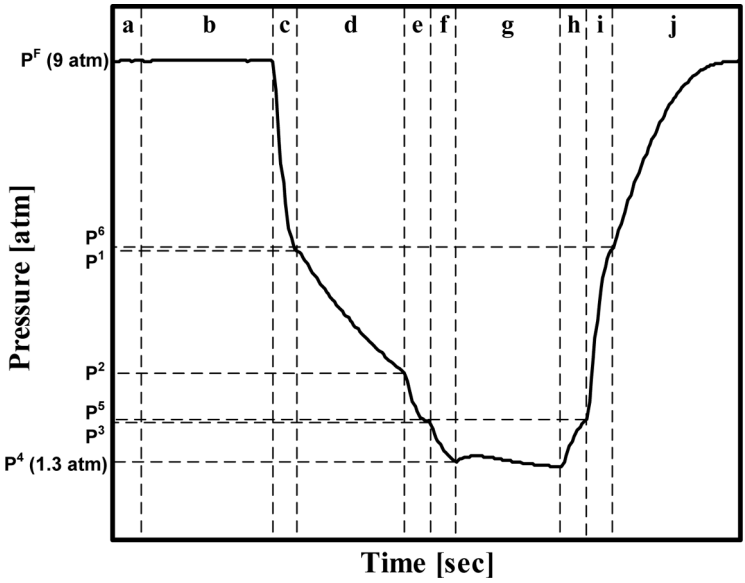

Figure 2. Pressure history.

Downloaded At: 09:02 25 January 2011

were adsorbed from the feed gas in step (a) and (b), which were afterwards desorbed and removed from the bed in steps (f) and (g). Steps (c) and (e) are added to recover and internally recycle a part of the void and co-adsorbed H_2 in the end of the bed. Step (d) also recovers a part of the void and the co-adsorbed H_2, and the recovery H_2 gas at this step is used as the purge gas of another bed. To obtain high product purity, the impurities are not allowed to break through the product end of the bed until the end of the second pressure equalization step (e). The effluent waste gases were produced during steps (f) and (g). The experimental operation conditions are summarized in Table 3. In every experimental run, the adsorption pressure and the purge pressure were set to 9 atm, and 1.3 atm, respectively.

MATHEMATICAL MODEL

The non-isothermal and non-adiabatic dynamic model, including mass, energy, and momentum balance was used to simulate a PSA process with the following assumption:

i. ideal gas law applies;
ii. the flow pattern can be described by the axial dispersion plug flow model;

Downloaded At: 09:02 25 January 2011

Table 2. Cycle steps for the PSA process

Cycle Times (sec)	$t_c/24$	$t_c/4$		$t_c/24$	$t_c/6$	$t_c/24$	$t_c/24$	$t_c/6$	$t_c/24$	$t_c/24$	$5t_c/24$	
Bed A	AD	AD & PP		EQI-BD	PP	EQII-BD	BD	PU	EQII-PR	EQI-PR	BF	
Bed B	EQI-PR	BF		AD	AD & PP		EQI-BD	PP	EQII-BD	BD	PU	EQII-PR
Bed C	BD	PU	EQII-PR	EQI-PR	BF		AD	AD & PP		EQI-BD	PP	EQII-BD
Bed D	EQI-BD	PP	EQII-BD	BD	PU	EQII-PR	EQI-PR	BF		AD	AD & PP	

t_c: total cycle time.

Table 3. Operating conditions in experimental run

Run	P^F [atm]	P^4 [atm]	v^{f*} [cm/s]	t_c [sec]
A	9	1.3	5.22	160
B	9	1.3	5.22	200
C	9	1.3	5.22	240
D	9	1.3	4.70	200
E	9	1.3	4.70	240
F	9	1.3	4.70	320
G	9	1.3	3.90	320
H	9	1.3	3.90	360
I	9	1.3	3.90	440
J	9	1.3	3.90	520
K	9	1.3	3.14	520
L	9	1.3	3.14	560
M	9	1.3	3.14	600

*Linear velocity.

Downloaded At: 09:02 25 January 2011

iii. the solid and gas phase reach thermal equilibrium instantaneously;
iv. the mass transfer rate can be represented by a linear driving force (LDF) rate expression; and
v. radial concentration and temperature gradients are negligible (11–19).

Based on the above assumptions, the mass balance for the bulk gas adsorption was written as follows:

$$-D_{Li}\varepsilon_b \frac{\partial^2 C_i}{\partial z^2} + \frac{\partial u C_i}{\partial z} + \varepsilon_t \frac{\partial C_i}{\partial t} + \rho_b \frac{\partial \bar{q}_i}{\partial t} = 0 \tag{1}$$

with the total bed voidage (ε_t) and the bed density (ρ_b) calculated by:

$$\varepsilon_t = \varepsilon_b + \varepsilon_p(1 - \varepsilon_b) \tag{2}$$

$$\rho_b = \rho_p\,(1 - \varepsilon_b) \tag{3}$$

The momentum balance in a bed was given by Ergun's equation:

$$\frac{dP}{dz} = -\left(\frac{150 \times 10^{-5}\mu_g(1-\varepsilon_b)^2}{4R_p^2{\varepsilon_b}^3}u + \frac{1.75 \times 10^{-5}M_w\rho_g(1-\varepsilon_b)}{2R_p\varepsilon_b^3}v_g^2\right) \tag{4}$$

Mass transfer rates are expressed as LDF model.

$$\frac{\partial \bar{q}_i}{\partial t} = k_i(q_i^* - \bar{q}_i) \tag{5}$$

Table 4. Dual-site Langmuir parameters and heat of adsorption

		k_1 [mmol/g]	k_2 [1/atm]	k_3 [K]	k_4 [mmol/g]	k_5 [1/atm]	K_6 [K]	Q_i [cal/mol]
Activated carbon	H_2	2.40E-5	9.0E-4	1700	4.80E-4	6.0E-5	1915	−1800
	CO	3.65E-3	8.7E-5	2003	4.37E-4	2.0E-3	2050	−4000
	CH_4	5.80E-3	1.0E-4	2060	7.40E-4	3.5E-3	2200	−5600
	CO_2	8.00E-3	8.0E-6	3100	1.40E-3	9.6E-7	4750	−5900
Zeolite 5A	H_2	7.8E-4	9.0E-5	1647	7.0E-6	1.2E-5	3000	−1500
	CO	2.3E-3	9.7E-5	2920	9.5E-4	7.9E-5	3280	−7000
	CH_4	2.6E-3	2.1E-4	2200	7.5E-4	3.0E-9	4800	−4600
	CO_2	3.0E-3	1.1E-3	2508	1.4E-3	1.0E-2	3300	−8500

Downloaded At: 09:02 25 January 2011

Assuming thermal equilibrium between fluid and particles, the energy balance for the gas and solid phase is given by:

$$-\varepsilon_b K_L \frac{\partial^2 T}{\partial z^2} + (\varepsilon_t \rho_g C_{pg} + \rho_B C_{ps}) \frac{\partial T}{\partial t} + \rho_g C_{pg} \varepsilon u \frac{\partial T}{\partial z} - \rho_B \sum_i^n Q_i \frac{\partial \bar{q}_i}{\partial t} + \frac{2h_i}{R_{B_i}} (T - T_W) = 0 \tag{6}$$

Energy balance around the wall of the column is represented as follows:

$$\rho_w C_{pw} A_w \frac{\partial T_w}{\partial t} = 2\pi R_{B_i} h_i (T - T_w) - 2\pi R_{B_o} h_o (T_w - T_{atm}) \tag{7}$$

where $A_w = \pi(R_{B_0}^2 - R_{B_i}^2)$.

The equilibrium isotherms are assumed to be described by Dual-Site Langmuir (DSL) model [7–8]:

$$q_i = \frac{q_{m_i 1} B_{i1} P y_i}{1 + \sum_k (B_{k1} P y_k)} + \frac{q_{m_i 2} B_{i2} P y_i}{1 + \sum_k (B_{k2} P y_k)} \tag{8}$$

where the isotherm parameters are functions of temperature:

$$q_{m1} = k_1,\ B_1 = k_2 \exp(k_3/T),\ q_{m2} = k_4,\ B_2 = k_5 \exp(k_6/T) \tag{9}$$

The DSL isotherm parameters and the values of heats of adsorption are listed in Table 4.

The boundary conditions for the PSA simulation are as follows:

$$\text{AD step}: y_i(0,t) = y_{i,F},\ T(0,t) = T_F,\ u(0,t) = u_F \tag{10}$$

$$\text{EQI-BD, PP and EQII-BD step}: u(0,t) = 0 \tag{11}$$

$$\text{BD step}: u(L,t) = 0 \tag{12}$$

$$\text{PG step}: y_i(L,t) = y_{i,PP},\ T(L,t) = T_F,\ u(L,t) = u_{PP}\frac{P_{PP}}{P_{PG}} \tag{13}$$

$$\text{EQII-PR and EQI-PR step}: y_i(L,t) = y_{i,EQ-BD},\ T(L,t) = T_F \tag{14}$$

$$\text{BF step}: y_i(L,t) = y_{i,P}, T(L,t) = T_F \tag{15}$$

The governing partial differential equations were solved in space and the resulting ordinary differential equations are solved using Aspen ADSIM from Aspen Technology Inc. (20).

Downloaded At: 09:02 25 January 2011

RESULTS AND DISCUSSION

Cyclic Steady State of PSA Process

In the PSA process, the cyclic steady state is important for the process analysis. It is determined that the changes of product purity, the concentration of the gas phase in the bed, and the temperature swing are almost constant. Doong et al. (1986) reached the cyclic steady state after 10 cycles for hydrogen separation of multi-component gas mixtures by the PSA process using the activated carbon (21). Lee et al. (1999) also reached the cyclic steady state after 10 cycles for hydrogen separation of coke oven gas (COG) by the two-bed PSA process.

Figure 3 shows behaviors of the product purity, which was obtained from the experiment for run A, F, and J. When the product purity is high (99.999%+), it is almost constant while the cycle number increased during run A. However, as the cycle number increased, the product purity decreased during runs F and J because the CO and CH_4 were exhausted at the end of the bed. For run F, the experiment reached the cyclic steady state after approximately 25 cycles. For run J, the experiment reached the cyclic steady state after approximately 20 cycles. In this study, the PSA process operated 30-cycles experiment.

Along with the product purity, the temperature variation in the bed represented a cyclic behavior of a PSA process. The temperature

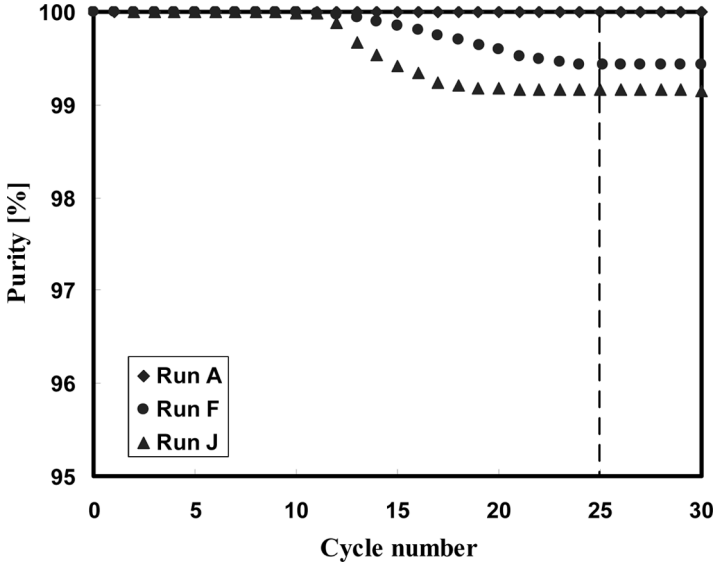

Figure 3. Product purity.

Downloaded At: 09:02 25 January 2011

variations at four locations of run F are presented in Fig. 4. It can be seen that a PSA process reached the cyclic steady state after 25 cycles, as revealed by the product purity (Fig. 3). The range of temperature swing was largest at the feed end section; this section behaved as the activated carbon layer where a considerable amount of adsorbates underwent adsorption and desorption during a cycle (19). However, the range of the temperature swing at the product end section was smallest because this section purified the raffinate stream from the activated carbon layer. It was noteworthy that the two thermocouples of 110 and 160 cm at the initial cycles showed a relatively small extent of temperature swing. This implies that, at an early stage of operation, the concentration wavefronts did not proceed much from the feed end due to the initial condition of the clean bed.

Effects of Total Cycle Time and Linear Velocity

The effect of total cycle time on the performance of a PSA process was studied with varying linear velocity under the adsorption pressure 9 atm. As shown in Fig. 5 (the linear velocity 5.2 cm/s), the product purity was high (99.999%+) until the total cycle time of 200 sec and then

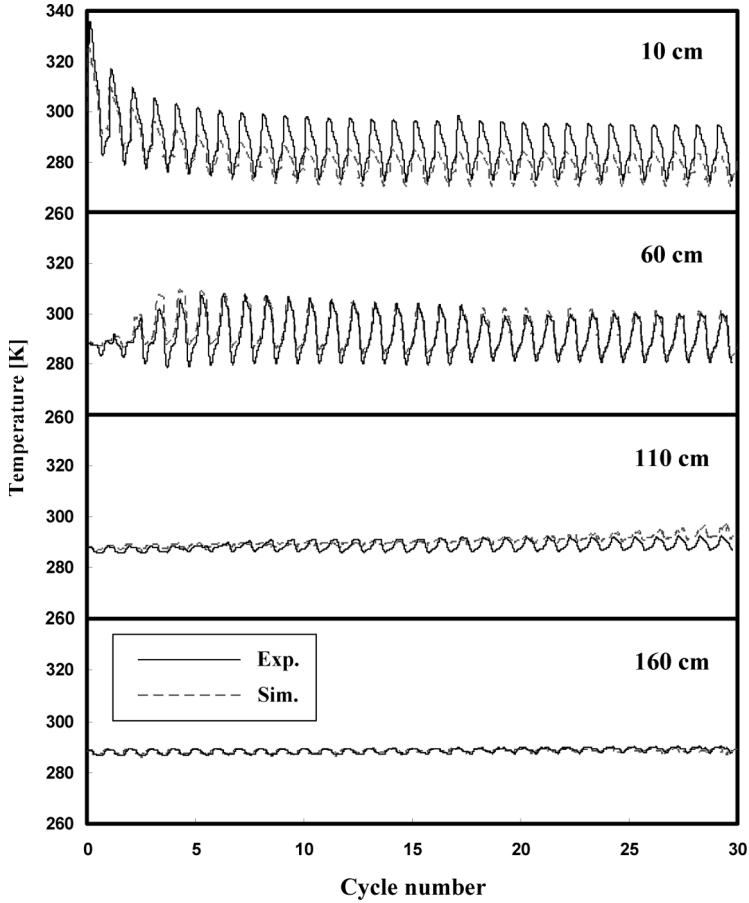

Figure 4. Transient variation of temperature at Run F.

decreased. A longer total cycle time resulted in lower product purities, as the bed was more contaminated. However, the recovery increased with increasing the total cycle time. This increase in the recovery results from a small amount of hydrogen remaining in the bed, as the bed was contaminated by the impurities. Figure 6 shows the concentration profiles in the gas phase at the end of the second pressure equalization step with different total cycle times. As the total cycle time increased, the mass transfer zones of impurity approached the end of the bed. Especially, as the total cycle time increased from 200 to 240 sec, the impurities, CO and CH_4, break through the product end of the column until the end of the last pressure equalization step. The recovery is lower (66.36%) in

Downloaded At: 09:02 25 January 2011

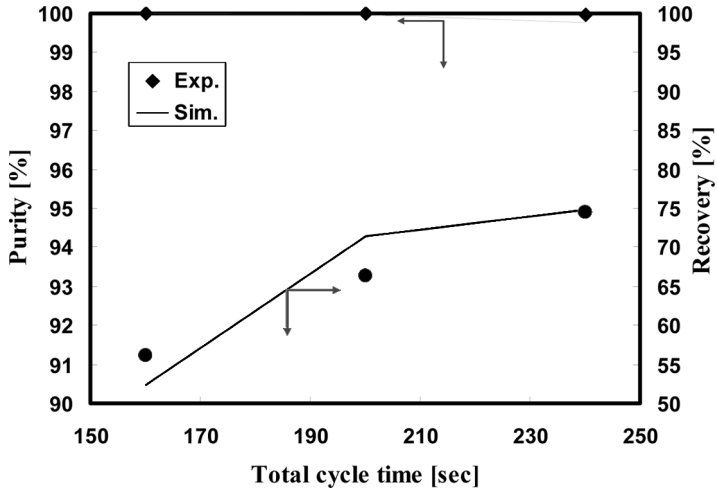

Figure 5. PSA process performance using different total cycle time at linear velocity 5.22 cm/s.

Downloaded At: 09:02 25 January 2011

order to obtain high product purity (99.999%+) at a linear velocity of 5.2 cm/s.

The recovery is important to operate the PSA process efficiently. To obtain the high recovery at the same process, the linear velocity must increase. However, as the linear velocity increases, the mass transfer zones of impurities are broadened so that the recovery decreases at the given purity (11). In order to obtain high recovery, the PSA process experimented with and simulated the various linear velocities and cycle times. The experimental results are shown in Figs. 7–9 with the simulation. With all the linear velocity, the trend of the purity and recovery was similar with increasing of the total cycle time. However, the recovery was different at high purity (99.999%+). When the linear velocity decreased from 5.2 to 4.7 cm/s, the recovery increased from 66.36 to 73.88% at high purity (99.999%+). The recovery increased from 73.88 to 75.93%, as the linear velocity decreased from 4.7 to 3.9 cm/s. But, the difference of the increasing of the recovery became smaller with decreasing the linear velocity. Also, when the linear velocity decreased from 3.9 to 3.14 cm/s, the recovery was similar 75.93% (3.9 cm/s), 75.43% (3.14 cm/s).

Effects of Residence Time

The design of the PSA process is complex because of the large number of variables and parameters involved, for example, the adsorbent type,

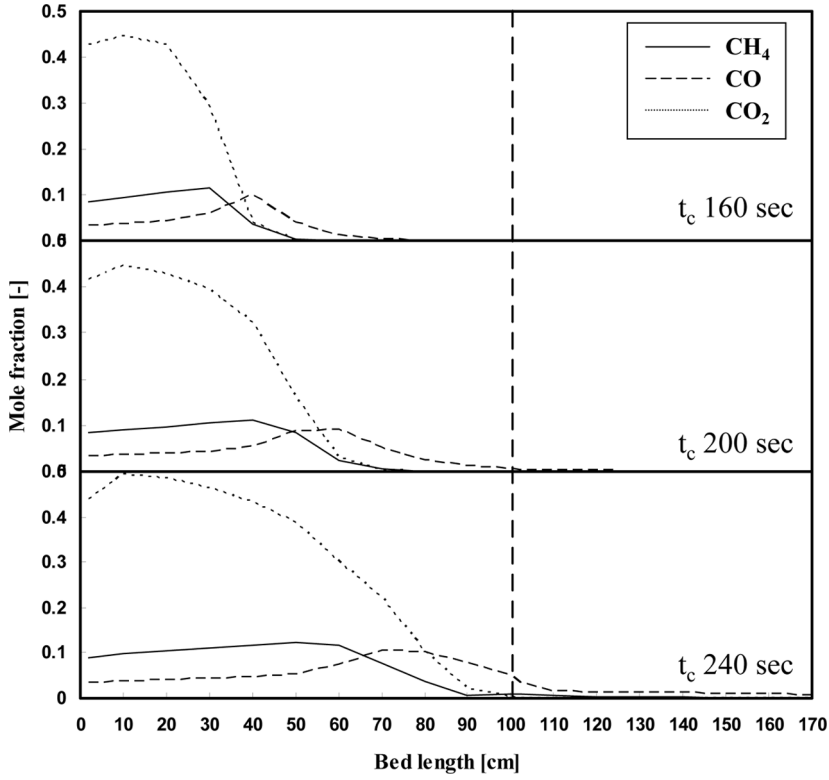

Figure 6. Concentration profiles in gas phase at the end of second pressure equalization step. (linear velocity: 5.22 cm/s)

the adsorbent particle size, the bed length/diameter ratio, the gas flow velocity, the residence time, the type of the PSA operating cycle, the duration of the steps in the PSA cycle, the number of beds, the feed gas pressure, the feed gas composition, the product purity, recovery, and the product throughput. When the adsorbents, the feed gas composition, and the operating condition, are given, the residence time is mainly the function for design of the PSA process. The residence time can be represented as:

$$\text{The residence time (RT)} = \frac{\text{bed volume}}{\text{feed flow rate}} \times \frac{\text{Adsorption pressure}}{\text{Atmosphere}} \quad (16)$$

If the residence time is too short, the bed has no significant adsorption. When sufficient residence time is provided, the desired product purity can be achieved. Increasing the residence time can be done

Downloaded At: 09:02 25 January 2011

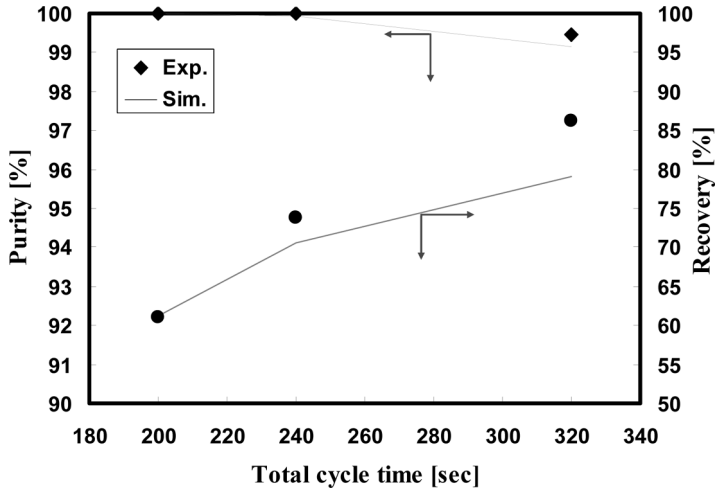

Figure 7. PSA process performance using different total cycle time at linear velocity 4.70 cm/s.

Downloaded At: 09:02 25 January 2011

by reducing the feed flow rate or by increasing the bed volume. Since the feed flow rate is determined by the desired capacity of the unit, the required residence time can be achieved by changing the bed volume. However, in an existing unit, residence time can be altered only by adjusting feed rate or feed pressure or both (6).

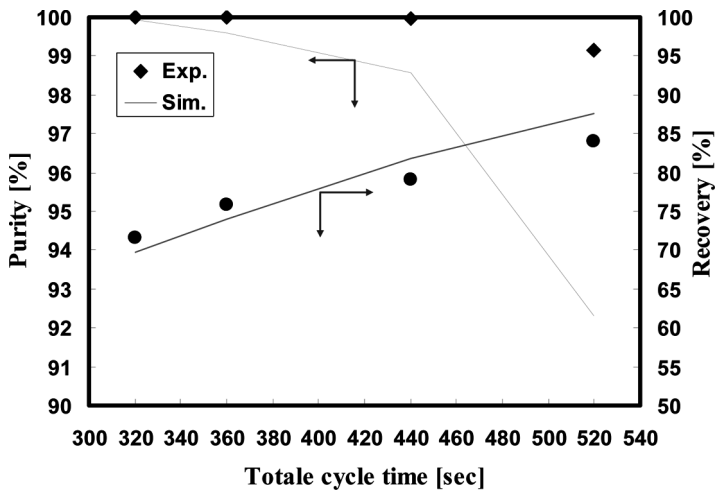

Figure 8. PSA process performance using different total cycle time at linear velocity 3.90 cm/s.

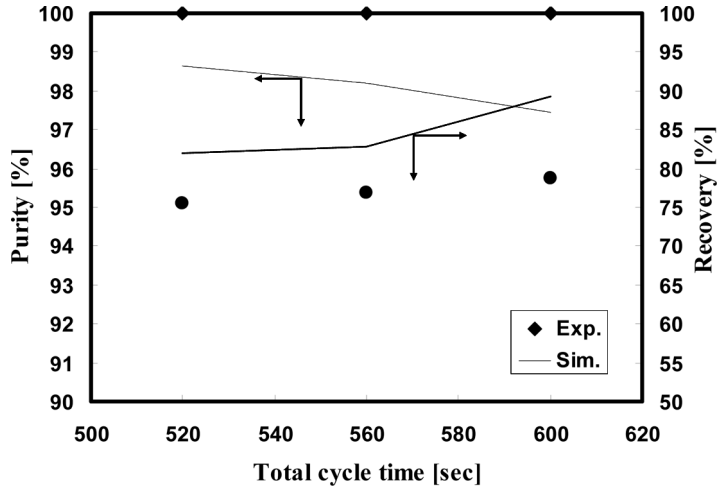

Figure 9. PSA process performance using different total cycle time at linear velocity 3.14 cm/s.

Figure 10 shows the experimental results obtained with different residence times with the desired product purity (99.999%+) when the bed volume and the adsorption pressure are fixed. The recovery increased about 8% when the residence time increased from 32.6 to 36.2 sec. The increase of the residence time means that the contact time between the

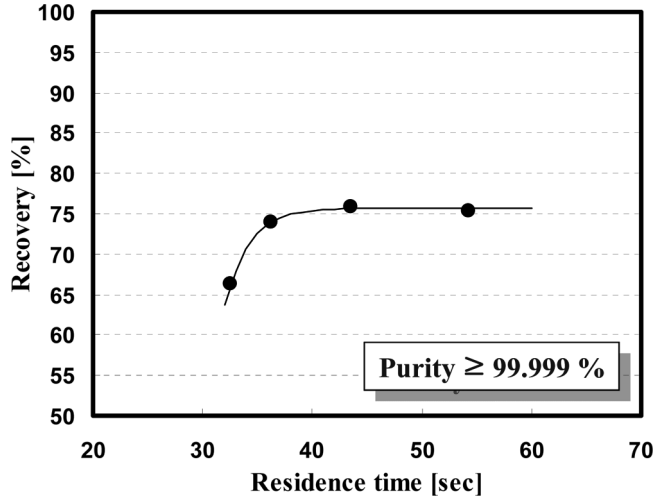

Figure 10. Recovery with the residence time at product purity 99.999%+.

Downloaded At: 09:02 25 January 2011

adsorbents and the impurities is increased. As the contact time is decreased in an existing PSA unit, the amount of the impurities through the adsorbents is increased due to increasing the feed flow rate. Thus, the mass transfer zones of impurities are broadened and the recovery is decreased at given product purity. On the other hand, the recovery increased about 2% when the residence time increased from 36.2 to 43.6 sec. Noteably, when the residence time increased from 43.6 to 54.2 sec, the recovery was not increased. This implies that the minimum residence time exists to obtain the maximum recovery at given product purity (99.999%+).

Figures 11–14 show the temperature variations at four location with different residence times. As the residence time increased from 32.6 to 43.6 sec, the range of temperature swing is larger at 60 cm of the section.

Downloaded At: 09:02 25 January 2011

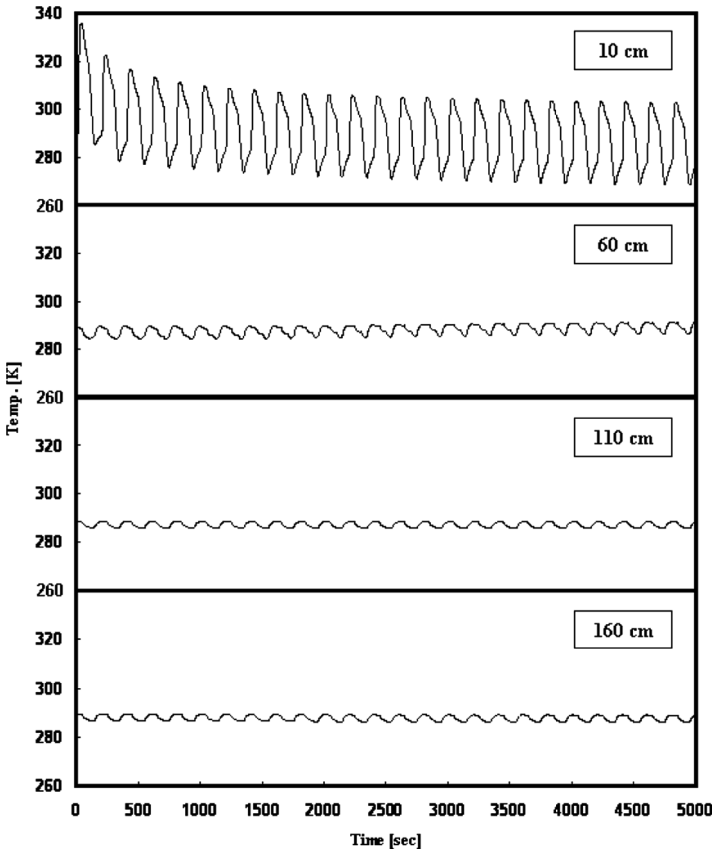

Figure 11. Transient variation of temperature at RT 32.6 sec.

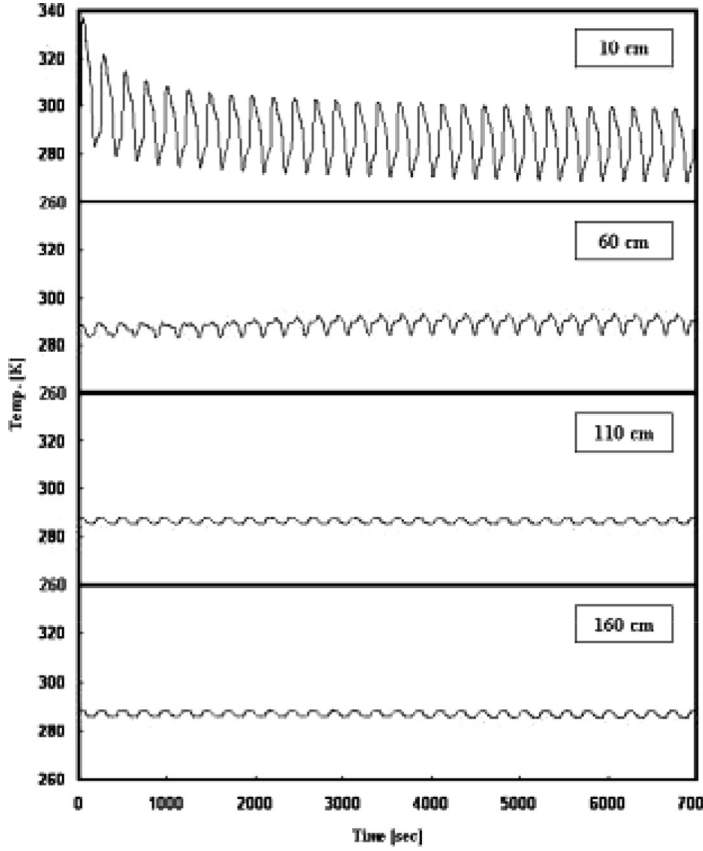

Figure 12. Transient variation of temperature at RT 36.2 sec.

Downloaded At: 09:02 25 January 2011

However, the range of temperature swing was similar when the residence time increased from 43.6 to 54.2 sec.

CONCLUSION

The four-bed, ten-step PSA process using a layered bed of activated carbon and zeolite 5A were studied to produce a high purity H_2 product from SMR off-gas. The non-isothermal, bulk separation PSA model adopted the linear driving force approximation for the particle uptake and the adsorption isotherm used the Dual-site Langmuir. It was possible to obtain hydrogen of 99.999% + purity with 75% + recovery.

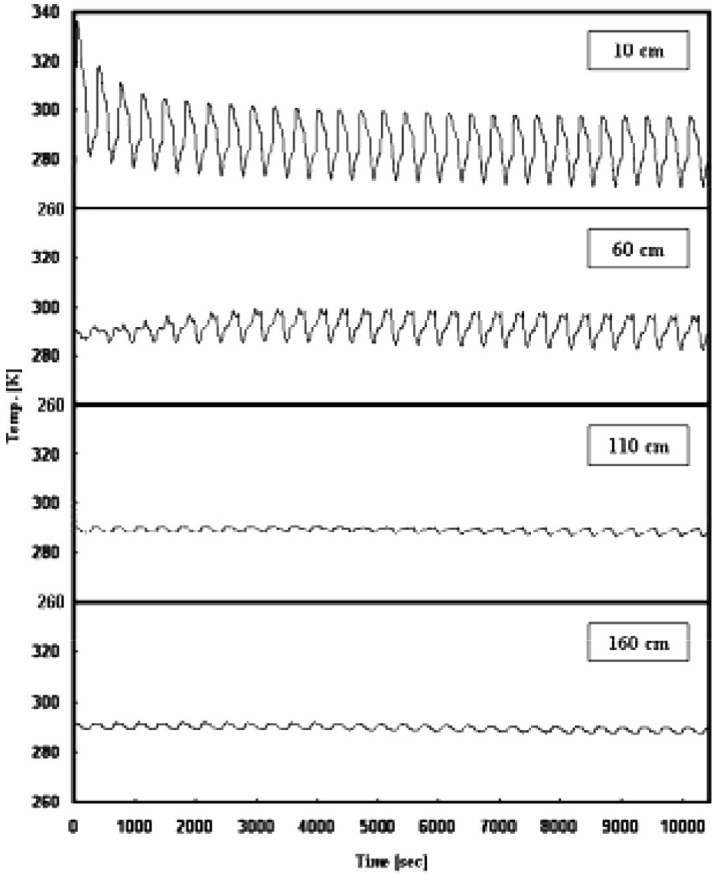

Figure 13. Transient variation of temperature at RT 43.6 sec.

When the total cycle time increased, the recovery increased. The product purity decreased because the impurities reached the product end of the bed and then broke through until the second pressure equalization step. With all the linear velocity, the trend of the purity and recovery was similar with the increase of total cycle time. However, at a desired product purity (99.999%+), the recovery increased with decreasing the linear velocity. The difference of the increasing of the recovery became smaller with the decreasing of the linear velocity. The recovery was similar 75% + less than 3.9 cm/s of the linear velocity.

When the adsorbents, the feed gas composition, and the operating condition are given, the residence time is mainly a function for design of the PSA bed size. The recovery increased with increasing the

Downloaded At: 09:02 25 January 2011

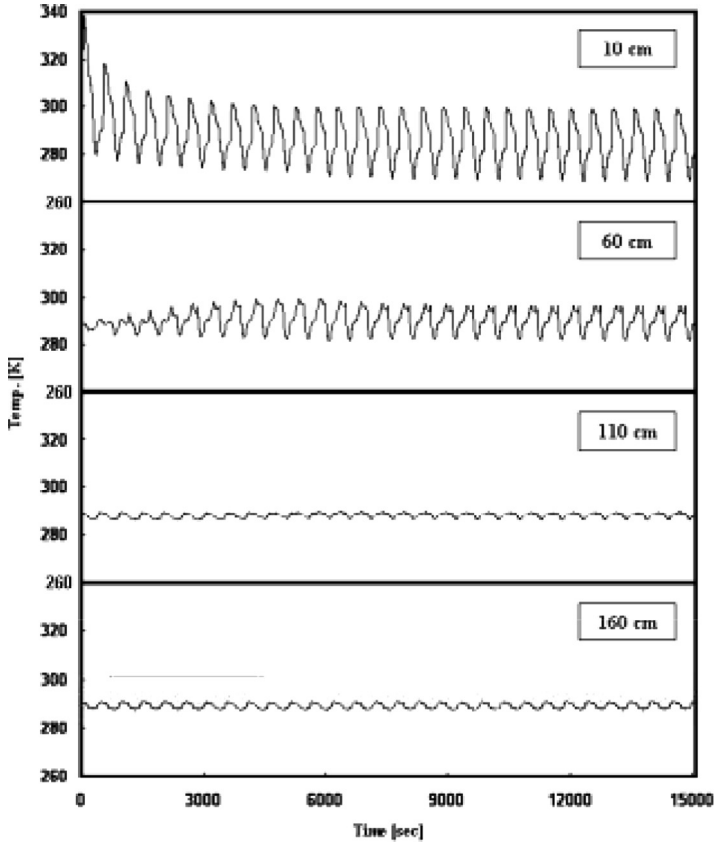

Figure 14. Transient variation of temperature at RT 54.2 sec.

residence time at given product purity because of the contact time between the impurities and the adsorbents is increased. The difference of increasing the recovery became smaller with increasing the residence time and then the recovery was not increased more than 43.6 sec of the residence time. The minimum residence time exists to obtain the maximum recovery at desired product purity.

ACKNOWLEDGMENT

This work was supported by SK Corporation and National RDND Organization for Hydrogen and Fuel Cell, Ministry of Commerce, Industry, and Energy.

Downloaded At: 09:02 25 January 2011

NOMENCLATURE

A_w	cross sectional area (cm^2)
C	gas phase concentration (mol/cm^3)
C_{pg}	heat capacity of gas phase (cal/mol·K)
C_{ps}	heat capacity of particle (cal/g·K)
C_{pw}	heat capacity of column wall (cal/g·K)
D_L	mass axial dispersion coefficient (cm^2/s)
h	heat transfer coefficient ($cal/cm^2 \cdot s \cdot K$)
K_L	thermal axial dispersion coefficient (cal/cm·s·K)
$k_{1\sim6}$	Dual-site Langmuir isotherm parameter
k_i	mass transfer coefficient (s^{-1})
P	pressure (atm)
$\bar{q}$	adsorbed amount (mol/g)
q^*	equilibrium amount adsorbed (mol/g)
Q	average isosteric heat of adsorption (cal/mol)
R_i	inner radius of column (cm)
R_o	outer radius of column (cm)
t	time (sec)
T	gas phase temperature (K)
T_{amb}	ambient temperature (K)
T_F	feed temperature (K)
T_w	wall temperature (K)
u	interstitial velocity (cm/s)
u_F	interstitial velocity of feed (cm/s)
y_i	mol fraction of ith component in the gas phase
z	axial position in the bed (cm)
ε_t	total bed voidage
ε_b	interparticle vodiage
ε_p	intraparticle voidage
μ	viscosity (cm/g·s)
ρ	density (cm^3/g)

Downloaded At: 09:02 25 January 2011

REFERENCES

1. Ruthven, D.M.; Farooq, S.; Knaebel, K.S. (1994) *Pressure Swing Adsorption*; VCH Publishers: New York.
2. Yang, R.T. (1987) *Gas Separation by Adsorption Process*; Butterworth: Boston, MA.
3. Sircar, S.; Waldron, W.E.; Rao, M.B.; Anand, M. (1999) Hydrogen production by hybrid SMR-PSA-SSF membrane system. *Sep. Purifi. Tech.*, *17*: 11.

4. Ahn, H.W.; Lee, C.H.; Seo, B.K.; Yang, J.Y.; Baek, K.H. (1999) Backfill cycle of a layered bed H_2 PSA process. *Adsorption*, *5*: 419.
5. Ruthven, D.M. (1984) *Principles of Adsorption and Adsorption Processes*; Wiley: New York.
6. Jain, S.; Moharir, A.S.; Li, P.; Wozny, G. (2003) Heuristic design of pressure swing adsorption: A preliminary study. *Sep. Purifi. Tech.*, *33*: 25.
7. Doong, S.J.; Yang, R.T. (1987) Hydrogen purification by the multibed pressure swing adsorption process. *Reactive Polymers*, *6*: 7.
8. Kumar, R. (1994) Pressure swing adsorption process: Performance optimum and adsorbent selection. *Ind. Eng. Chem. Res.*, *33*: 1600.
9. Kumar, R.; Guro, D.E.; Schmidt, W.P. (1995) A new concept to increase recovery from H_2 PSA: Processing different pressure feed streams in a single unit. *Gas. Sep. Pruifi.*, *9*: 271.
10. Sircar, S.; Golden, T.C. (2000) Purification of hydrogen by pressure swing adsorption. *Sep. Sci. Tech.*, *35*: 667.
11. Park, J.H.; Kim, J.N.; Cho, S.H. (2000) Performance analysis of four-bed H_2 PSA process using layered beds. *AIChE Journal*, *46*: 790.
12. Waldron, W.E.; Sircar, S. (2000) Parametric study of a pressure swing adsorption process. *Adsorption*, *6*: 179.
13. Ahn, H.W.; Yang, J.Y.; Lee, C.H. (2001) Effects of feed composition of coke oven gas on a layered bed H_2 PSA process. *Adsorption*, *7*: 339.
14. Choi, B.U.; Nam, G.M.; Choi, D.K.; Lee, B.K.; Kim, S.H.; Lee, C.H. (2004) Adsorption and regeneration dynamic characteristics of methane and hydrogen binary system. *Korean J. Chem. Eng.*, *21*: 821.
15. Biegler, L.T.; Jiang, L.; Fox, V.G. (2004) Recent advances in simulation and optimal design of pressure swing adsorption systems. *Sep. Purifi. Rev.*, *33*: 1.
16. Cen, P.; Yang, R.T. (1986) Bulk gas separation by pressure swing adsorption. *Ind. Eng. Chem. Fundam.*, *25*: 758.
17. Yang, J.Y.; Lee, C.H.; Chang, J.W. (1997) Separation of hydrogen mixtures by a two-bed pressure swing adsorption process using zeolite 5A. *Ind. Eng. Chem. Res.*, *36*, 2789.
18. Yang, J.Y.; Lee, C.H. (1998) Adsorption dynamics of a layered bed PSA for H_2 recovery from coke oven gas. *AIChE Journal*, *44*: 1325.
19. Lee, C.H.; Yang, J.Y.; Ahn, H.W. (1999) Effects of carbon-to zeolite ratio on layered bed H_2 PSA for coke oven gas. *AIChE Journal*, *45*, 535.
20. Aspen (2003) *Aspen Custom Modeler: Modeling Language Reference Guide*; Aspen Technology Inc.: Cambrige.
21. Doong, S.J.; Yang, R.T. (1986) Bulk separation of multicomponent gas mixture by pressure swing adsorption: Pore/surface diffusion and equilibrium models. *AIChE Journal*, *32*, 397.

Downloaded At: 09:02 25 January 2011